Elastic responses of wind-tracing floating offshore wind turbines

Lamei, Azin; Hayatdavoodi, Masoud; Riggs, H. Ronald

Published in:
Proceedings of the 37th Int. Workshop on Water Waves and Floating Bodies (IWWWFB), April 10--13, 2022, Giardini Naxos, Italy

Publication date:
2022

Elastic Responses of Wind-tracing Floating Offshore Wind Turbines

Azin Lamei[a], Masoud Hayatdavoodi[a,b] and H. Ronald Riggs[c]

a. School of Science and Engineering, University of Dundee, Dundee DD1 4HN, UK
b. College of Shipbuilding Engineering, Harbin Engineering University, Harbin, China
c. Civil and Environmental Engineering Dep., University of Hawaii, Honolulu, Hawaii 96822, USA

Email: alamei@dundee.ac.uk

This study is concerned with the motion analysis and structural responses of a multi-unit floating offshore wind turbine to combined wave and wind loads. Three wind turbines are placed on an equilateral triangular platform. A single-point mooring system is used to allow the structure to rotate in response to the environmental loads. Hydrodynamic and aerodynamic loads are determined by use of the linear diffraction theory and the blade element momentum method, respectively and the elastic response of the entire structure is determined by use of a finite element analysis. The responses of the fully flexible structure to co-directional and misaligned wind and wave loads are studied.

Introduction

Floating platforms that can support multiple wind turbines are introduced to potentially reduce the cost of floating offshore wind turbines. While placing multiple turbines on the same floating structure may reduce costs compared to multiple individual platforms, it adds to the complexities associated with the motion analysis and elastic response of the system to the environmental loads. In this study, a numerical approach is presented to obtain the elastic motions of multi-unit floating offshore wind turbines (FOWTs) to combined wind and wave loads. Here, a multi-unit wind-tracing triangular platform is considered. The platform consists of three pontoons and three columns at the corners, shown in Fig. 1 (a). Three 5 MW NREL wind turbines are installed on top of each column. To minimize the wake effects on the trailing wind turbine, the distance between each hub centre of the rotors is set to $2.2\,D_r = 277.2\ m$, where D_r is the rotor diameter. The draft of the structure is $d = 16\ m$. The structure is moored to the seabed with a single-point mooring system. A submerged turret bearing is located under the pontoons. Three taut cables connect the bottom of the columns of the platform to the turret and the turret is connected to the seabed with four catenary mooring lines. The turret can be located in an infinite number of horizontal and vertical locations under the platform. In an optimization study for the specific platform design, the preferred location of the turret is 64 m under SWL, along the x-axis and 40.05 m away from the trailing column. Further details about this concept can be found in Li et al. (2019).

A numerical tool is developed for aeroelasticity and hydroelasticity analysis of FOWTs in the frequency domain. The structural analysis of the entire FOWT is carried out with the finite element method. The aerodynamic loads on the rotors are obtained with blade element momentum method, and linear diffraction wave theory is used for the hydrodynamic loads on the floating structure. Herein, responses of the rigid and flexible structures to wave loads are determined and compared. Then, responses of the fully flexible structure to combined wind and wave loads for various incoming wave directions are obtained.

Combined Wave and Wind Impact on Elastic Bodies

A FOWT is typically under simultaneous effect of wind, wave and current loads and the mooring forces of the structure. The presented approach only considers the effect of wind and wave loads and the mooring forces of the FOWT. Hydrodynamic loads on the FOWT platform is computed by the linear wave diffraction theory. The total load on a floating structure is given by the sum of external hydrodynamic pressure force, hydrostatic restoration forces and mooring line loads. Linear hydroelasticity analysis is based on extending the rigid body degrees of freedom with generalized modes to include the deformation of the body. The mode shapes of the structure are obtained with the finite element method and the displacement of the structure is expressed with a reduced modal basis. In this case, the hydrostatic stiffness includes the change in the hydrostatic pressure and the structural geometric stiffness. The complete formulation developed by Huang & Riggs (2000) is applied. In the absence of wind loads, the equation of motion of the elastic body is written as

$$\xi_j[-\omega^2(M_{ij} + a_{ij}) + i\omega(\,b_{ij}) + (\,c_{ij,moor} \,+\, c_{ij})] \;=\; AX_i, \quad i,j = 1,2,\cdots m, \tag{1}$$

where $6 \leq m$ is the number of generalized modes, M_{ij} is the modal structural mass matrix, and a_{ij}, b_{ij} and c_{ij} are the added mass, hydrodynamic damping and hydrostatic stiffness coefficient matrices, respectively. Moreover, $c_{ij,moor}$ is the stiffness matrix of the mooring lines. X_i is the amplitude of wave excitation force divided by the wave amplitude A and is presented in complex form, ω is the wave frequency and ξ_j is the complex body response phasor in mode j.

The aerodynamic loads on the rotor is computed by the steady blade element momentum method. For a FOWT, the total thrust force on the rotor depends on the relative motion of the platform

$$T(V_{rel}) = \frac{1}{2}\rho A_r C_T(V_{rel}^2), \tag{2}$$

where ρ is the air density, A_r is the rotor projected area, and C_T is the thrust coefficient. The relative incoming wind speed on the rotor, V_{rel}, is defined as $V_{rel} = V_0 - V_h$, where V_0 is the incoming wind speed on a fixed rotor, and V_h is the speed of the hub centre, along the direction of the incoming wind. In frequency domain, V_h is expressed as $i\omega(\xi_1 + \xi_5(z_h - z_{cg}))$, where z_h and z_{cg} are the vertical coordinates at the hub and the centre of gravity. For a FOWT, assuming that the structure speed at the tower top, V_h is small, the thrust force with relative incoming wind speed, Eq. (2) can be approximated by Taylor series,

$$T(V_{rel}) = \frac{1}{2}\rho A_r C_T(V_0^2) - \rho A_r C_T(V_0\ i\omega(\xi_1 + \xi_5(z_h - z_{cg}))). \tag{3}$$

where the second order and higher terms are discarded. In Eq. (3), the first term represents the thrust force on a fixed tower and it is assumed that it is an excitation force in surge acting at the top of the structure by the incoming wind. The wind force is harmonic and with the same frequency as the incident waves, and the wind direction is always orthogonal to the rotor, parallel to the x-direction. We assume that the integrated aerodynamic normal force over the blades act at the hub centre and eventually is transferred to the tower top. Hence, we can obtain the wind load phase angle following the same approach as in MacCamy & Fuchs (1954) for wave-interaction with a circular cylinder i.e.

$$F_{1,W} = \frac{1}{2}C_T\rho V_0^2 A_r \cos(\omega t - \delta_{\text{aero}}), \tag{4}$$

where $F_{1,W}$ is the thrust force on a fixed rotor in surge and δ_{aero} is the phase angle of the inline force and it is determined as

$$\delta_{\text{aero}}(kr_0) \ = \ -\tan^{-1}\big[\frac{Y_1^{'}(kr_0)}{J_1^{'}(kr_0)}\big], \tag{5}$$

in which, k is the wave number, $J_p(kr)$ and $Y_p(kr)$ are the Bessel functions of the first and the second kind of order p, respectively, and r_0 is the top diameter of the tower. Furthermore, the second term in Eq. (3) can be rewritten as $i\omega(\xi_1 + \xi_5(z_h - z_{cg}))\rho C_T V_0$, where $\rho C_T V_0$ represents an aerodynamic damping coefficient, B_{aero}, for a FOWT. The total aerodynamic load vector acting on the centre of gravity, F_W is the sum of the wind load on the rotor and the tower calculated following a similar approach. The wind load vector, F_W, and the aerodynamic damping matrix, $B_{aero,mat}$ on the rotor are added to right-hand side and the left-hand side of the the equation of motion of a floating platform in frequency domain, Eq. (1), respectively. To determine the responses of a FOWT to combined wind and wave loads we have,

$$\xi_j[-\omega^2(M_{ij} + a_{ij}) + i\omega(\ b_{ij} + \ B_{aero,mat}\ ) + (\ c_{ij,moor}\ +\ c_{ij})] \ = \ AX_i \ + \ F_W\ , \quad i,j = 1,2,\cdots m. \tag{6}$$

The computations of the wind-tracing platform are carried out in HYDRAN-XR, (NumSoft Technologies 2020). HYDRAN-XR is a potential-flow solver integrated with finite element analysis and can consider single and multi-unit floating offshore wind turbines. HYDRAN-XR has been enhanced to include the wind loads on single and multi-unit FOWT

Here, rather than applying the total wind force at the hub centre as indicated above, the aerodynamic load is applied across the front face of the blades. Likewise, the wind load on the tower is distributed on its area facing the inflow wind. In aerodynamic analysis, the normal wind force on the annular control volumes over the blades are computed and distributed over the front face nodes of the rotor. Similarly, the aerodynamic damping coefficient is obtained with local thrust coefficients on each control volume and assigned to the front nodes of the blades. The final wind load vector, F_W, and aerodynamic damping matrix on the centre of gravity of the structure is obtained and added to the equation of motion of the FOWT in frequency domain. The equation of motion is solved for the translational and rotational modes of the structure together with the generalized modes, accounting for aeroelasticity and hydroelasticity of the FOWT.

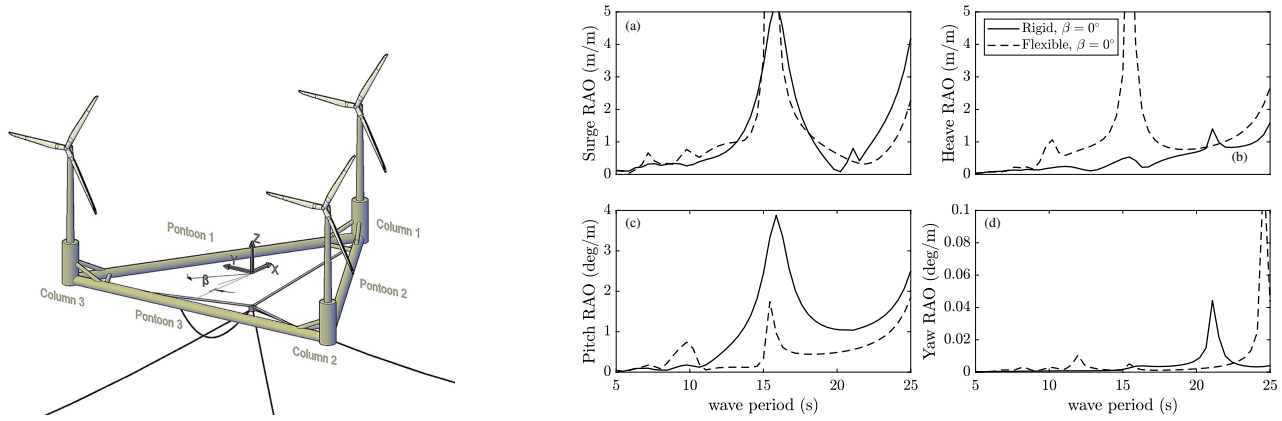

Figure 1: (a) Schematic of the wind-tracing multi-unit FOWT and (b) comparison of RAOs of the rigid and flexible structures to waves with $\beta = 0°$, in the absence of wind.

Results and Discussion

Results are presented in three parts, namely (i) comparison of the rigid and flexible responses to wave loads (in the absence of wind), (ii) comparison of the responses of a SPAR FOWT to combined wind and wave loads with laboratory measurements and (iii) responses of the flexible structure to combined wind and wave loads for several incoming wave directions.

An earth-fixed Cartesian coordinate system is chosen with its origin on the still water level, and z-axis pointing upwards in the positive direction. The translation motions, surge (ξ_1), sway (ξ_2), and heave (ξ_3), are parallel to the x-, y- and z-axes, respectively and the rotational motions, roll(ξ_4), pitch (ξ_5), and yaw (ξ_6), are about the x-, y- and z-axes, respectively.

The response amplitude operators (RAOs) of the wind-tracing FOWT are computed for the rigid and flexible structures. The RAOs in surge, heave, pitch and yaw for the rigid and flexible structures are compared over the wave period in headseas, $\beta = 0°$ in Fig. 1(b).

The surge RAOs of both rigid and flexible wind-tracing FOWTs are approximately similar over the wave period. However, the rigid structure undergoes larger pitch RAOs compared with the flexible body. Moreover, a new peak at approximately 15 s is introduced to the heave RAOs when the flexibility of the wind-tracing FOWT is included. The yaw RAOs of both rigid and flexible structures are approximately zero except at $T = 22$ s and $T = 24$ s, where a peak is computed for the rigid body and the flexible body, respectively.

Next, the motions of a 5 MW SPAR FOWT to waves and steady wind loads are computed and compared with laboratory measurements conducted by Ahn & Shin (2017). The laboratory experiments are carried out for a model with a scaling ratio of 1 : 128 with waves and rated wind speed of the 5 MW wind turbine, 11.4 m/s. The SPAR FOWT is moored with three catenary mooring lines in 320 s water depth and a draft of 120 m. The FOWT is modelled with respect to the prototype dimensions and its RAOs in surge, heave and pitch are compared with laboratory measurements by Ahn & Shin (2017) in Fig. 3. In general, an excellent agreement is observed between the numerical results by HYDRAN-XR and the laboratory measurements.

Finally, wind- and wave-induced responses of the fully flexible wind-tracing FOWT is computed in the frequency domain for co-directional and misaligned wind and wave loads. In our approach, with steady blade element momentum method, it is assumed that the incoming wind is always orthogonal to the rotors. Thus, the misalignment of wind and waves are modelled by varying the incoming wave direction. The wind load on the towers and the rotors of the wind-tracing FOWT is computed at wind speed 11.4 m/s. Figure 3 presents the RAOs of the wind-tracing FOWT in its rigid body modes for wave heading angles $\beta = 0°$, $45°$, $90°$ and $135°$, and wave periods from 5 s to 25 s. Shown in Fig. 3, heave RAOs do not change significantly by increasing the wave heading angles. However, in surge and pitch, RAOs with $\beta = 0°$ are larger than the responses with higher wave heading angles. Moreover, surge and pitch RAOs are both at their minimum with $\beta = 90°$. Furthermore, the wind-tracing FOWT experience largest motions in sway, roll and yaw when the wind load direction is perpendicular to the incoming wave

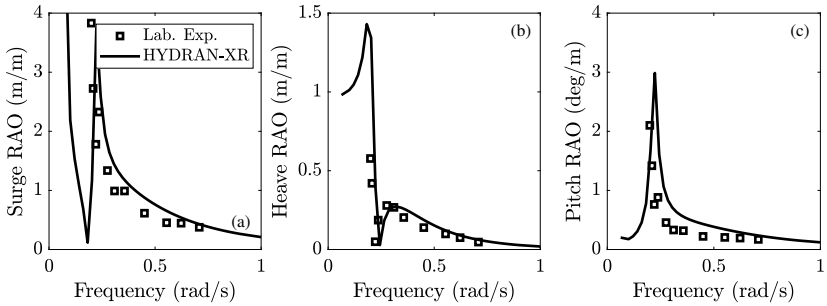

Figure 2: Comparison of the wave-induced RAOs of the SPAR FOWT computed by HDYRAN-XR and the laboratory measurements of Ahn and Shin (2017).

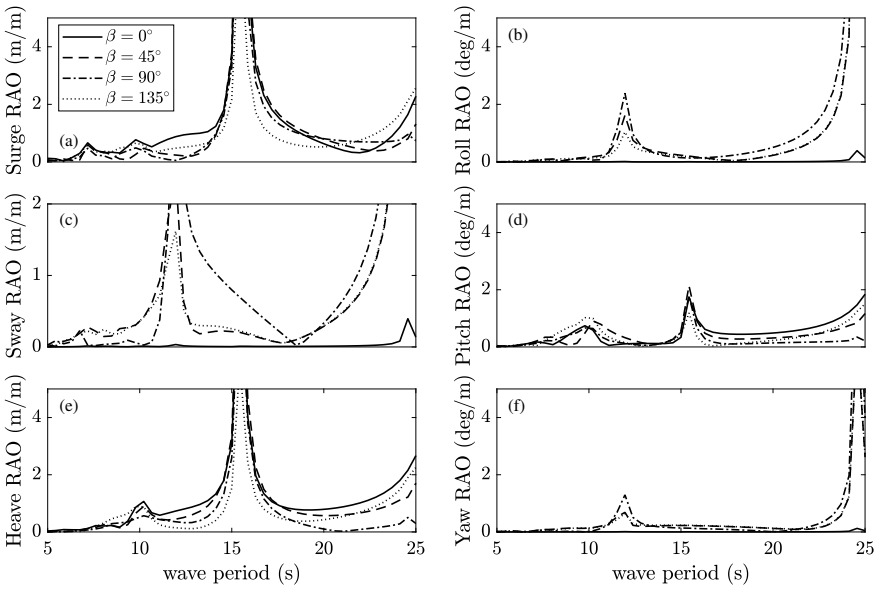

Figure 3: RAOs of the wind-tracing FOWT for codirectional and misaligned wind and wave loads, with wave heading angles $\beta = 0°$, 45°, 90° and 135°.

loads, *i.e.* $\beta = 90°$

Acknowledgement This work is partially funded by the CBJ-Ocean Engineering of Hong Kong.

References

Ahn, H. J. & Shin, H. (2017), 'Model test and numerical simulation of OC3 spar type floating offshore wind turbine', *International Journal of Naval Architecture and Ocean Engineering* **11**(1), 1–10.

Huang, L. L. & Riggs, H. R. (2000), 'The hydrostatic stiffness of fexible foating structures for linear hydroelasticity', *Marine Structures* **13**, 91–106.

Li, S., Lamei, A., Hayatdavoodi, M. & Wong, C. (2019), Concept design and analysis of wind-tracing floating offshore wind turbines, *in* 'Proceedings of the ASME 2019 2nd International Offshore Wind Technical Conference, November 3-6, St. Julian's, Malta', ASME, pp. 1–8.

MacCamy, R. & Fuchs, R. (1954), *Wave forces on piles: A diffraction theory*, Tech. Memo. No. 69, Beach Erosion Board. Army Corps of Engineers, 1-17.

NumSoft Technologies (2020), HYDRAN-XR, hydrodynamic response analysis with integrated structural finite element analysis, version 20.1, Technical report, Numsoft Technologies.